

# NASA Technical Memorandum 86260

## STRUCTURAL PERFORMANCE OF ORTHOGONAL TETRAHEDRAL TRUSS SPACE-STATION CONFIGURATIONS

JOHN T. DORSEY

JULY 1984

**NASA**

National Aeronautics and  
Space Administration

**Langley Research Center**  
Hampton, Virginia 23665

# STRUCTURAL PERFORMANCE OF ORTHOGONAL TETRAHEDRAL SPACE-STATION CONFIGURATIONS

John T. Dorsey  
July 1984

## INTRODUCTION

The Structural Concepts Branch at Langley Research Center has recently been studying structural configurations for very large solar arrays that can be used for the proposed permanent U.S. space-station. Approximately 40,000 ft<sup>2</sup> of solar arrays are required to meet the eventual power demands of 150 kw for the station. These very large solar arrays should have sufficient stiffness such that an elaborate on-orbit control system is not required for the space-station. A fundamental frequency greater than 0.4 hz for the complete space-station has been chosen as a design goal to meet the stiffness requirement. The solar array support structure should also be compatible with existing technology for deployable solar blankets (ref. 1), and the power array must be capable of modular growth over the lifetime of the space station.

A space-station concept, consisting of a central collection of modules and two solar wing arrays, which satisfies the considerations mentioned in the preceding paragraph is described in detail in reference 2. By using a three longeron triangular truss-beam with a bay size of 200 in. to support the solar arrays, a fundamental frequency of .403 hz was achieved for the complete space-station. The solar arrays would be supported from two sides of the triangular beam and thermal radiators would be supported by the third side. Astronauts would construct the complete solar wing array with the aid of a mobile erector which moves internally along the truss-beam like an elevator.

Changing the solar array support truss beam from a triangular cross-section to the square cross-section of the orthogonal tetrahedral truss results in several significant design benefits. For example, an orthogonal tetrahedral truss beam with one more side would allow the mobile erector to travel on the outside of the beam, while leaving two sides to support solar arrays and one to support thermal radiators. The orthogonal tetrahedral solar wing array concept is described in reference 3. The reference also gives a detailed description of a machine which can assist in erecting the truss-beam as well as several space station configurations which could be erected using the same machine.

In this paper, the dynamic characteristics of the orthogonal tetrahedral truss wing and two space-station concepts which incorporate the wing are presented. The first space-station concept studied has a central platform and two solar wing arrays. The central platform provides a place to attach the various space-station modules, as well as a platform where orbital transfer vehicles can be serviced and where large antennas can be constructed. (See reference 3). The second space station studied consists of a central keel and two solar wing arrays. Attaching all of the modules, orbital transfer vehicles, etc. to the bottom of this keel allows the space station to fly in a gravity gradient stabilized mode.

The final studies reported in this paper deal with individual strut failures in the orthogonal tetrahedral truss wing. One important advantage the four longeron truss has over the three longeron triangular-truss is the redundancy provided by the fourth longeron. Failure of any of the members in the triangular-truss would cause a mechanism to form in the wing at that location and thus constitute failure of the wing. Because of the inherent redundancy in the orthogonal tetrahedral truss design, however, failure of a truss member would only result in reduced strength and stiffness in the wing, not a catastrophic failure as in the triangular truss. In the final studies presented, critical members are identified in the

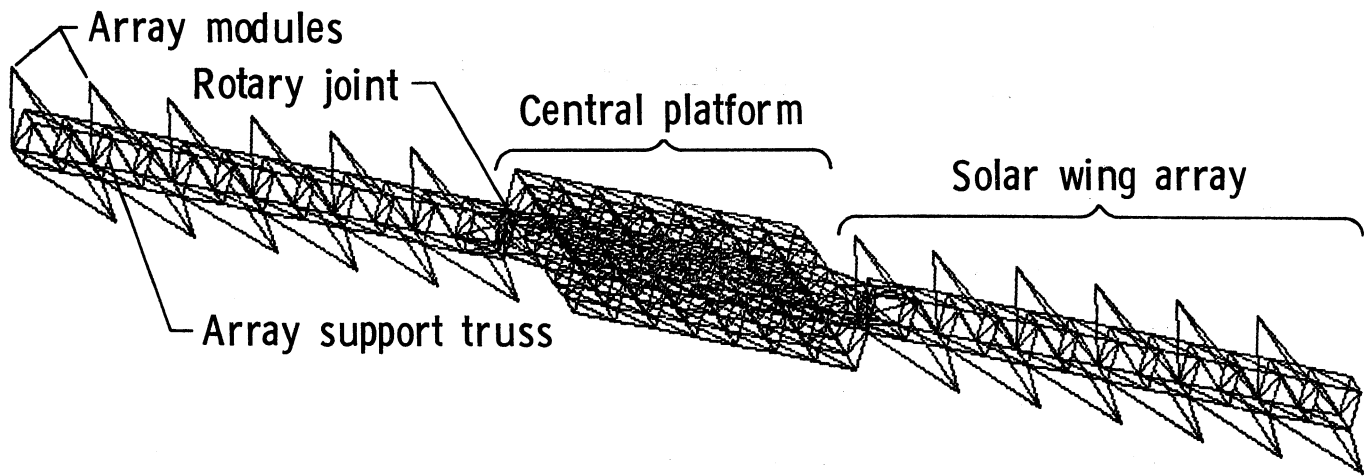
orthogonal tetrahedral truss wing for applied tip loadings. These critical members are then removed from the model and the resulting effects on wing strength and stiffness are assessed.

## Figure 1

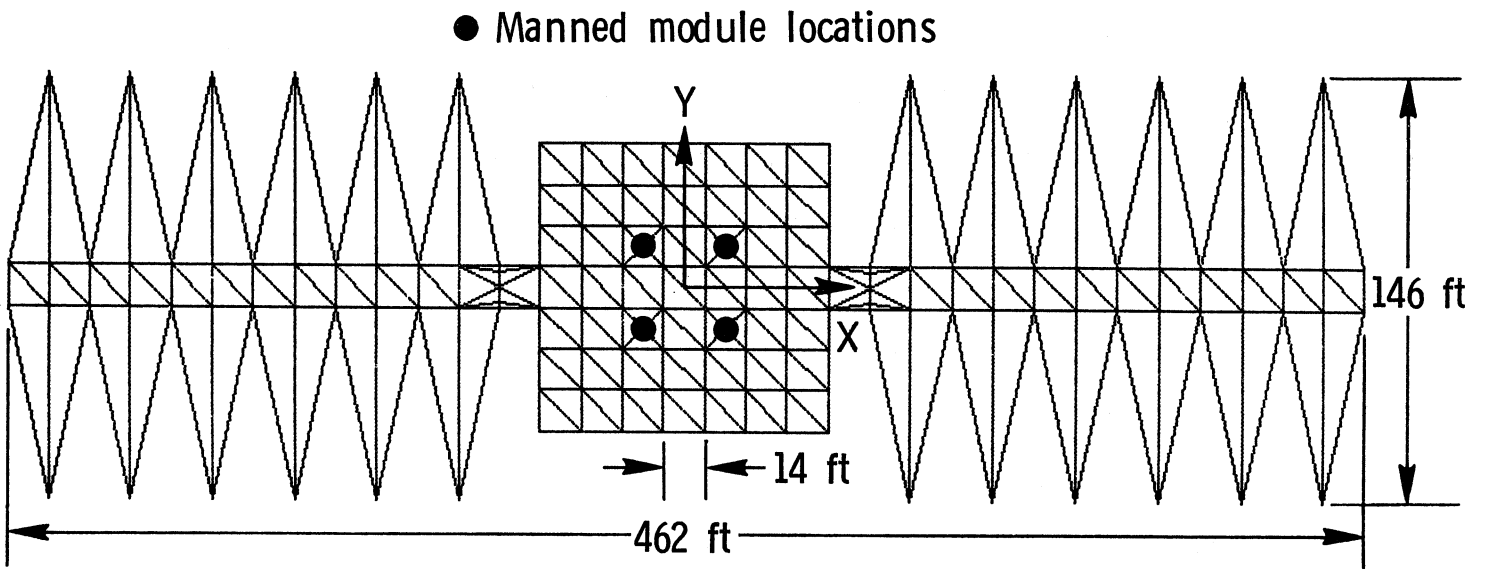
### CENTRAL PLATFORM/SOLAR WING ARRAY SPACE-STATION

The first space-station studied consisted of a central platform and two solar wing arrays. (See figure 1). Both the platform and the solar array support truss are constructed using the orthogonal tetrahedral truss described in reference 3. The large rotary joints which attach the solar wing arrays to the platform allow the solar cells to track the sun as the space-station orbits the Earth.

The space-station dimensions, as given in figure 1b, are for a fully mature 150 kw station. All of the bays in this space-station are 14 ft square. The central platform has seven bays on a side with four modules attached to the upper surface at the locations shown in the figure. Each of the wing arrays has twelve bays in the support truss and are sized to provide 75 kw of power to the station. The total length of the space-station is 462 ft, and the total width is 146 ft.



a. Space - station components



b. Space - station dimensions

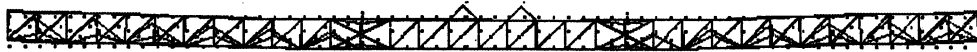
Figure I. Central platform/ solar wing array space-station.

Figure 2

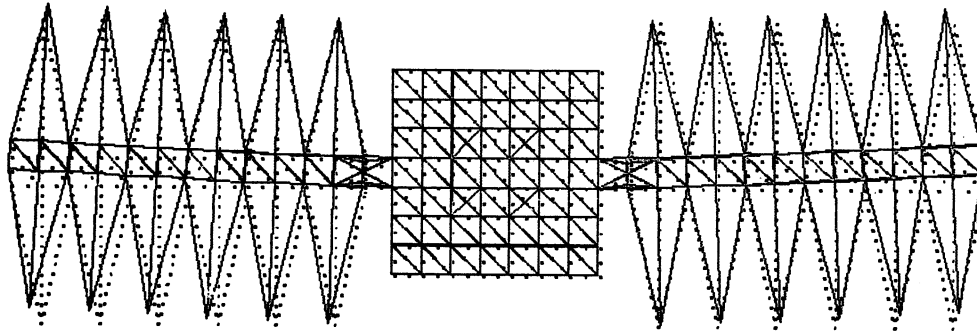
MODE SHAPES FOR CENTRAL PLATFORM/SOLAR WING ARRAY  
SPACE-STATION WITH FOUR 50 000 LBM MODULES

The finite element model shown in figure 1 was used to determine the frequencies and mode shapes of the space-station for two cases. In the first case, no modules were attached to the platform and in the second case, four 50,000 lbm modules were attached to the platform in the locations shown. The modules were represented in the model by point masses attached to the platform by rigid members. The struts used to model both the platform and array support truss are 2 in. graphite-epoxy tubes with an area of  $.3657 \text{ in}^2$  and a modulus of  $40 \times 10^6 \text{ lbf/in}^2$ . Rigid masses representing nodal cluster mass were also included in the model for each joint in the platform and array support truss. The mass of each rotary joint was assumed to be 2000 lbm and added to appropriate nodes in the wing array. Finally, the mass of the 24 individual array modules, as described in reference 2, were also included in the model.

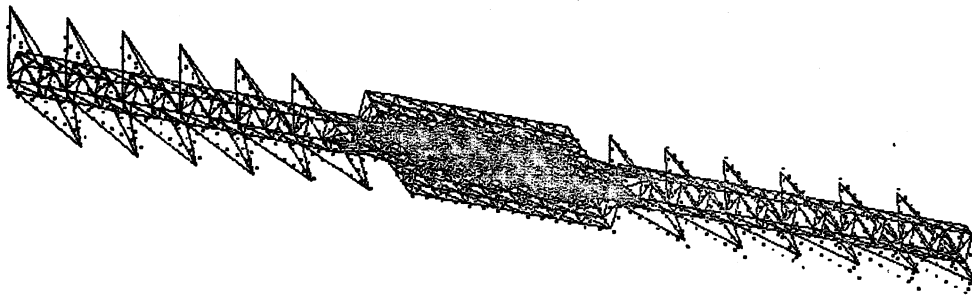
Figures 2a - 2d illustrate the first four elastic mode shapes obtained when four 50,000 lbm modules are included in the finite element model. The first six modes are rigid body and have zero eigenvalues. The first two flexible body modes, shown in figures 2a and 2b, are first symmetric bending of the wing arrays about the X and Z axes, respectively. Because of the large module mass on the platform, the wing arrays act similarly to two cantilevers vibrating off of the stationary platform. The next two modes are antisymmetric and symmetric torsion of the two wing arrays about the X axis. In mode 9, the platform acts as a node (point of zero rotation) between the two arrays whereas in mode 10, the platform rotates as a rigid body in a direction opposite to the two arrays.



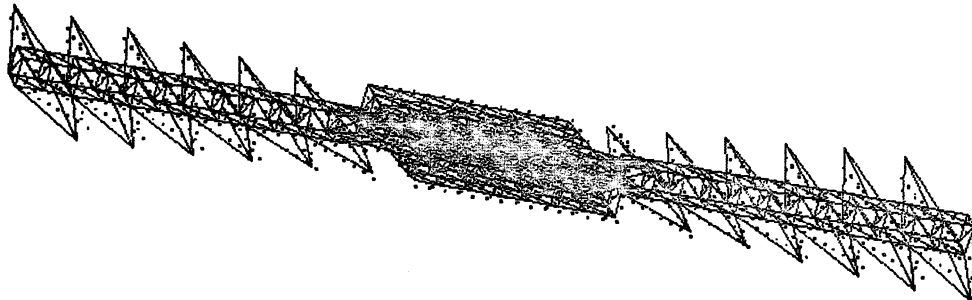
a. Mode 7 - first symmetric solar array bending about X.



b. Mode 8 - first symmetric solar array bending about Z.



c. Mode 9 - first antisymmetric solar array torsion about X.



d. Mode 10 - first symmetric solar array torsion about X.

Figure 2. Mode shapes for central platform/solar wing array space-station with four 50 000 lbm modules.



Table I

COMPARISON OF THE CENTRAL PLATFORM/SOLAR WING ARRAY  
SPACE STATION WITH\* AND WITHOUT MODULES

In Table I, the structural characteristics of the Central Platform/Solar Wing Array space-station are compared when modules are and are not attached to the platform. When the four modules are added to the space-station, the fundamental frequency drops by 9.7% from .558 hz to .504 hz, and the fundamental mode changes from first torsion to first bending about the Y axis. The mode shape is given by the short hand notation in parentheses next to each frequency. Here; one stands for first, two for second etc.; T stands for torsion, and B for bending; the X, Y, Z and 45 subscripts indicate about which axis the bending or torsion is taking place. The table also shows how adding four 50,000 lbm modules affects the space-station moments of inertia, giving a 117% increase in  $I_{xx}$ , an 11% increase in  $I_{yy}$  and an 18% increase in  $I_{zz}$ . These changes in space-station moments of inertia will have an effect on the rigid body dynamics and controllability of the space station.

[\* Four Modules at 50,000 lbm each]

TABLE I.  
COMPARISON OF THE CENTRAL PLATFORM/SOLAR  
WING ARRAY SPACE STATION WITH\* AND WITHOUT MODULES

	Without Modules	With Modules
Frequency, hz		
f <sub>1</sub> - f <sub>6</sub>	.0	.0
f <sub>7</sub>	.558 (1T <sub>x</sub> )	.504 (1B <sub>y</sub> )
f <sub>8</sub>	.676 (1B <sub>z</sub> )	.526 (1B <sub>45</sub> )
f <sub>9</sub>	.749 (1B <sub>y</sub> )	.604 (1T <sub>x</sub> )
f <sub>10</sub>	.903 (2T <sub>x</sub> )	.711 (2T <sub>x</sub> )
Total Mass, lbm	22 700	222 700
Moment of Inertia+, $\frac{\text{lbf-in}^2}{\text{in/sec}^2}$		
I <sub>xx</sub>	.138 x 10 <sup>8</sup>	.300 x 10 <sup>8</sup>
I <sub>yy</sub>	.148 x 10 <sup>9</sup>	.164 x 10 <sup>9</sup>
I <sub>zz</sub>	.162 x 10 <sup>9</sup>	.191 x 10 <sup>9</sup>
I <sub>xy</sub>	-.131 x 10 <sup>5</sup>	-.131 x 10 <sup>5</sup>
I <sub>xz</sub>	-.921 x 10 <sup>4</sup>	-.921 x 10 <sup>4</sup>
I <sub>yz</sub>	-.737 x 10 <sup>4</sup>	-.737 x 10 <sup>4</sup>

\* Four Modules at 50,000 lbm each.

+ Multiply by g = 386 in/sec<sup>2</sup> to get weight inertias.

Figure 3

150 KW GRAVITY GRADIENT STABILIZED SPACE-STATION TRUSS MODEL

The second space-station configuration studied consists of a long central truss keel and two solar wing arrays, as shown in figure 3. As in the first space-station configuration discussed, the bays here are 14 ft square and the struts forming the structure have an area of  $.3657 \text{ in}^2$  and a modulus of  $40 \times 10^6 \text{ lbf/in}^2$ . There are 26 bays in the keel, and the two wing arrays are attached at the seventh bay down from the top. Two extra bays have been added to the wing arrays in this model. Thus, a hinge can be built just outboard of the rotary joint on each wing. A rigid body rotation about the hinge allows the solar arrays to correct for beta-angle effects between the incident solar vector and the solar arrays. When nonstructural components such as modules, fuel tanks and orbital transfer vehicles (OTV's) are placed at the tip of the keel farthest away from the solar arrays, this configuration can fly gravity gradient stabilized. These components, however, were not included in this model of the station.

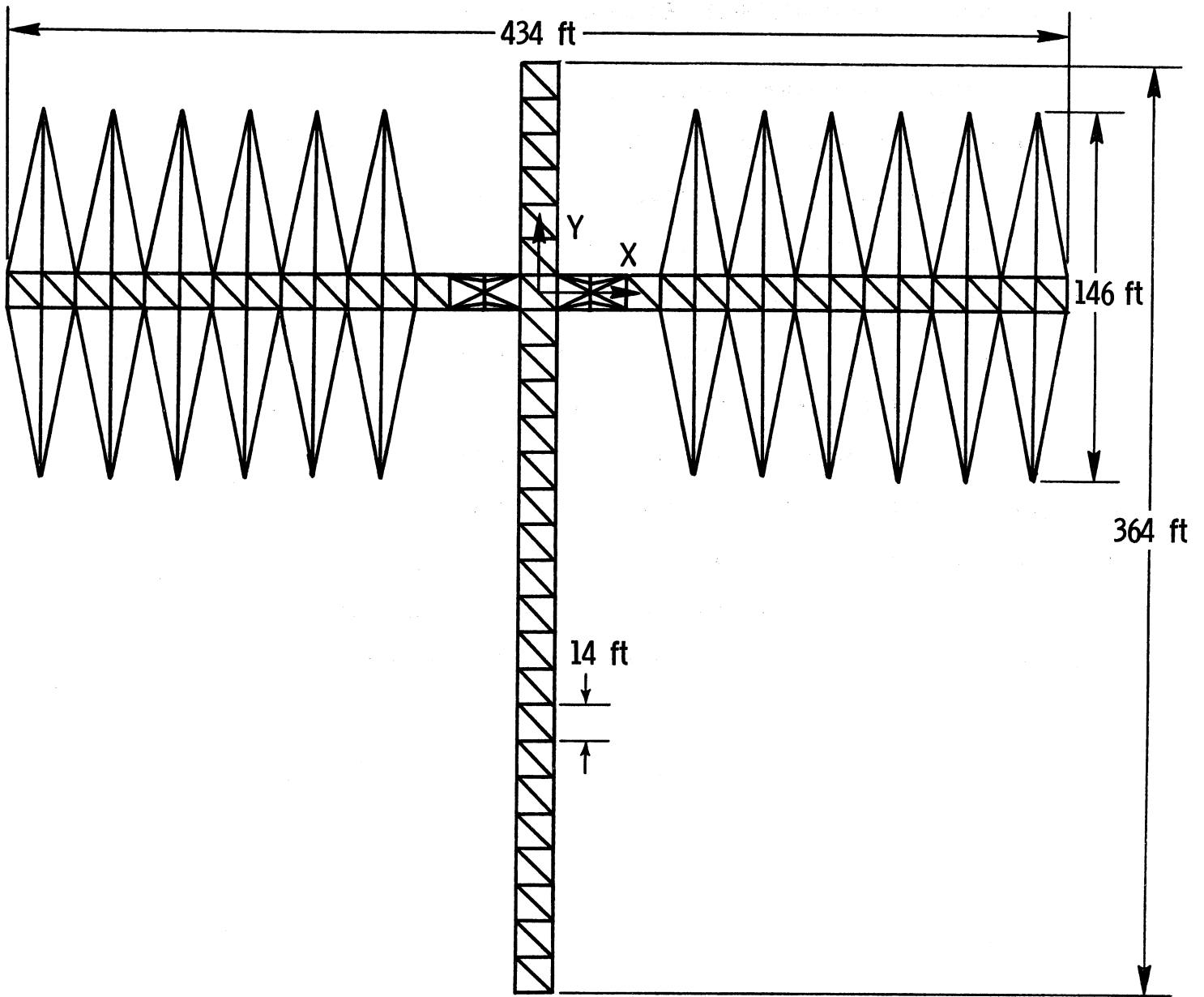


Figure 3. 150 kw gravity gradient stabilized space-station truss model.

## Figure 4

### 150 KW GRAVITY GRADIENT STABILIZED SPACE-STATION EQUIVALENT BEAM MODEL

Figure 4 shows an equivalent beam/rigid mass representation of the truss model discussed in figure 3. The EI, GJ, EA and mass per length etc. of the beams making up the equivalent beam model were calculated, using expressions derived in reference 4, to give the equivalent properties for a 14 ft. orthogonal tetrahedral truss. Also shown in the figure are components which would form a complete 150 kw space station. These components (which are discussed in some detail later) are represented in the model by rigid masses, with appropriate moments of inertia, attached to the ends of rigid beams. The radiators are located near the top of the tower, three sets of module clusters are half way between the arrays and the tower bottom, and the OTV hangers and propellant tank are near the bottom of the tower. The exact location of these various items would be determined such that the space-station would fly gravity gradient stabilized.

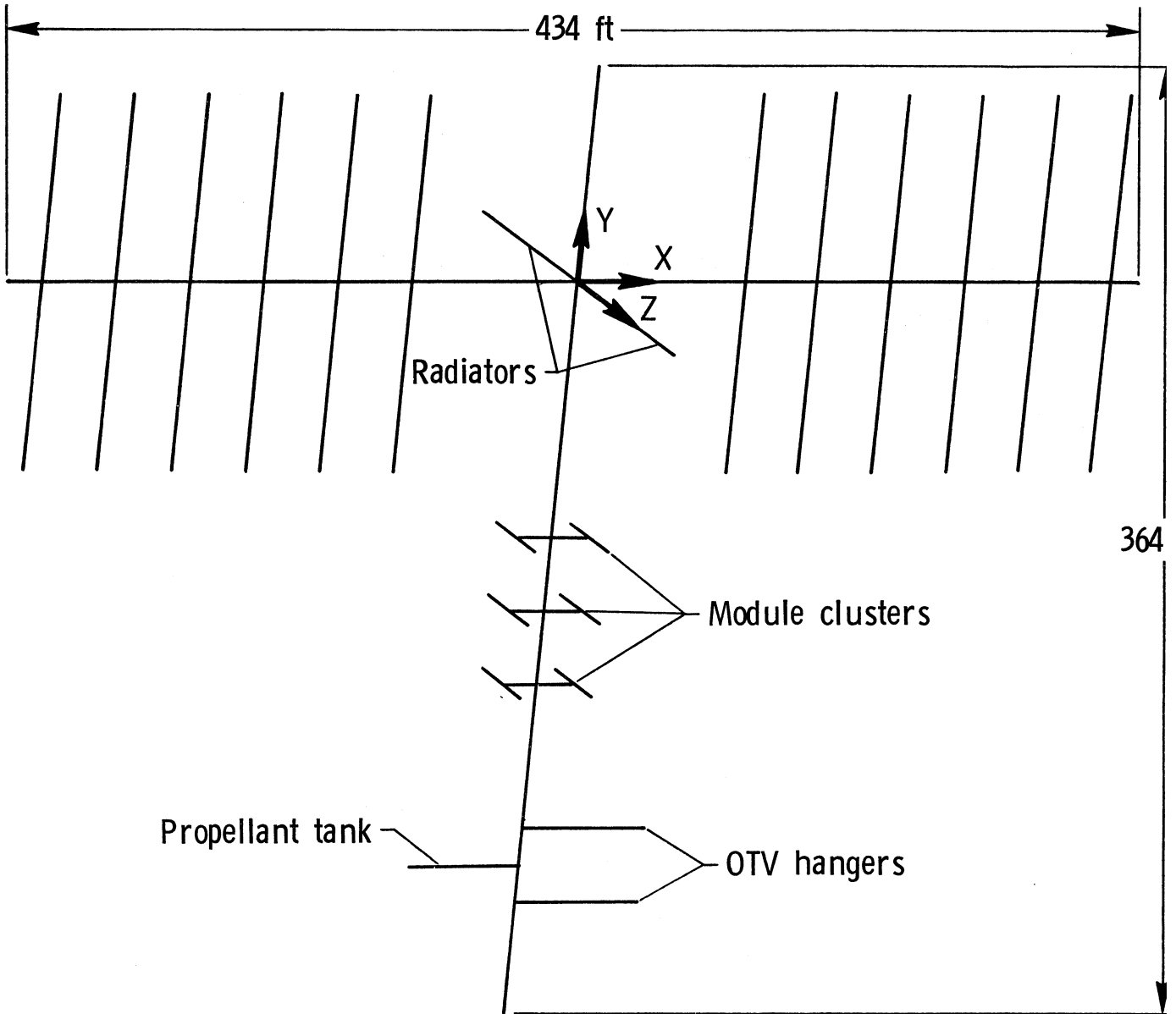


Figure 4. 150 kw gravity gradient stabilized space-station equivalent beam model.

Table II

COMPARISON OF FULL TRUSS AND EQUIVALENT BEAM GRAVITY  
GRADIENT STABILIZED SPACE-STATIONS

In Table II, the structural characteristics of the full truss and equivalent beam models are compared for the case where nonstructural components (radiators, module clusters, OTV hangers, and OTV fuel tank) are not included in the station. A comparison is also given for the equivalent beam model with all components included. The comparison between the full truss and equivalent beam models, without components, serves to validate the equivalent beam model which was used for subsequent studies. The frequencies associated with the first four elastic modes are very close for the two models with the largest difference being in the tenth mode where the frequency for the equivalent beam model is 3.3% greater than the frequency for the truss model. The only difference in mode shapes is in the ninth mode where the equivalent beam model has pure first wing bending about the Z axis ( $1WB_z$ ) and the full truss model has first wing bending about the Z axis plus first tower bending about the X axis. For the notation in this table, W stands for wing, T with a subscript is torsion about the subscript axis, and T without the subscript is tower. Thus, for example,  $1TT_y$  is first tower torsion about the y axis. Very good agreement is also obtained between the two models for the total mass, and mass moments of inertia. The addition of 325 000 lbm of nonstructural components causes a considerable drop in the first four elastic frequencies as well as a change in mode shapes. Substantial increases in mass moments of inertia also occur when the components are added to the station with  $I_{xx}$  becoming 12 times as large,  $I_{yy}$  1.6 times as large, and  $I_{zz}$  3.1 times as large.

TABLE II.

COMPARISON OF FULL TRUSS AND EQUIVALENT BEAM GRAVITY  
GRADIENT STABILIZED SPACE STATIONS

Frequency, hz	Full Truss Model Without Components*	Equivalent Beam Model Without Components	Equivalent Beam Model With Components
f <sub>1</sub> - f <sub>6</sub>	.0	.0	.0
f <sub>7</sub>	.504 (1WT <sub>x</sub> )	.512 (1WT <sub>x</sub> )	.187 (1TT <sub>y</sub> )
f <sub>8</sub>	.601 (1TB <sub>x</sub> )	.610 (1TB <sub>x</sub> )	.266 (1TB <sub>z</sub> )
f <sub>9</sub>	.624 (1TB <sub>x</sub> +1WB <sub>z</sub> )	.616 (1WB <sub>z</sub> )	.381 (1TB <sub>x</sub> )
f <sub>10</sub>	.733 (1WB <sub>y</sub> )	.757 (1WB <sub>y</sub> )	.469 (2TT <sub>y</sub> )
Total Mass, lbm	22 000	21 600	347 000
Moment of Inertia+, $\frac{\text{lb-in}^2}{\text{in/sec}^2}$			
I <sub>xx</sub>	.263 x 10 <sup>8</sup>	.262 x 10 <sup>8</sup>	.326 x 10 <sup>9</sup>
I <sub>yy</sub>	.119 x 10 <sup>9</sup>	.115 x 10 <sup>9</sup>	.178 x 10 <sup>9</sup>
I <sub>zz</sub>	.145 x 10 <sup>9</sup>	.141 x 10 <sup>9</sup>	.440 x 10 <sup>9</sup>
I <sub>xy</sub>	-.958 x 10 <sup>4</sup>	.0	-.971 x 10 <sup>7</sup>
I <sub>xz</sub>	.728 x 10 <sup>4</sup>	.0	.0
I <sub>yz</sub>	-.109 x 10 <sup>4</sup>	.0	.0

\* Components are Radiator, Modules, OTV Hangers, and Fuel Tank.

+ Multiply by g = 386 in/sec<sup>2</sup> to get weight inertias.



### Table III

#### MASS AND MOMENT OF INERTIA DATA FOR GRAVITY GRADIENT STABILIZED SPACE-STATION COMPONENTS

The mass and moment of inertia data for the various components added to the station structure to form a complete 150 kw space station are contained in Table III. The location of these various items is shown in figure 4. The mass moment of inertia data were obtained by assuming that the module cluster, OTV hangers, and fuel tank were hollow cylinders, while the radiator was a flat plate. The total mass of these components is 326,000 lbm, which, when added, brings the total mass of the space-station up to 348,000 lbm.

TABLE III

MASS AND MOMENT OF INERTIA DATA FOR GRAVITY  
GRADIENT STABILIZED SPACE-STATION COMPONENTS

Component Name	Number Added to Model	Mass, lbm (each)	$\frac{I_{xx,*}}{\text{lb-ft-in}^2}$ $\frac{\text{in}}{\text{sec}^2}$	$\frac{I_{yy,*}}{\text{lb-ft-in}^2}$ $\frac{\text{in}}{\text{sec}^2}$	$\frac{I_{zz,*}}{\text{lb-ft-in}^2}$ $\frac{\text{in}}{\text{sec}^2}$
Module Cluster	6	50 000.	$3.47 \times 10^6$	$3.47 \times 10^6$	$9.15 \times 10^5$
OTV Hanger	2	8 520.	$3.19 \times 10^5$	$1.85 \times 10^6$	$1.85 \times 10^6$
Fuel Tank (Empty)	1	6 600.	$1.21 \times 10^5$	$1.06 \times 10^6$	$1.06 \times 10^6$
Radiator	2	1 000.	$3.91 \times 10^5$	$7.77 \times 10^4$	$7.77 \times 10^4$

\* Moments of inertia given in the space-station global coordinate frame.

Figure 5

VARIATION IN THE GRAVITY GRADIENT STABILIZED SPACE-STATION  
FREQUENCIES DUE TO ROTATION OF THE SOLAR WING ARRAYS

The variation of the first four elastic frequencies of the station as the solar wing arrays are rotated are presented in this figure. The zero angle position is shown in figure 4 where the solar arrays lie in the X-Y global plane. When the wings are rotated to a 90° angle, the solar arrays will lie in the global X-Z plane.

At the zero angle position, the fundamental frequency,  $f_7$ , is .187 hz and the mode is first torsion of the tower. This fundamental frequency is only 37% of the fundamental frequency of the station without all of the components added. The other frequencies at zero wing angle are  $f_8 = .266$  hz (first bending of the tower about the Z axis),  $f_9 = .381$  hz (first bending of the tower about the X axis) and,  $f_{10} = .469$  hz (first wing torsion about the X axis). The frequencies shown vary only slightly as the solar wing arrays are rotated with the largest variation, 3%, occurring in  $f_8$ .

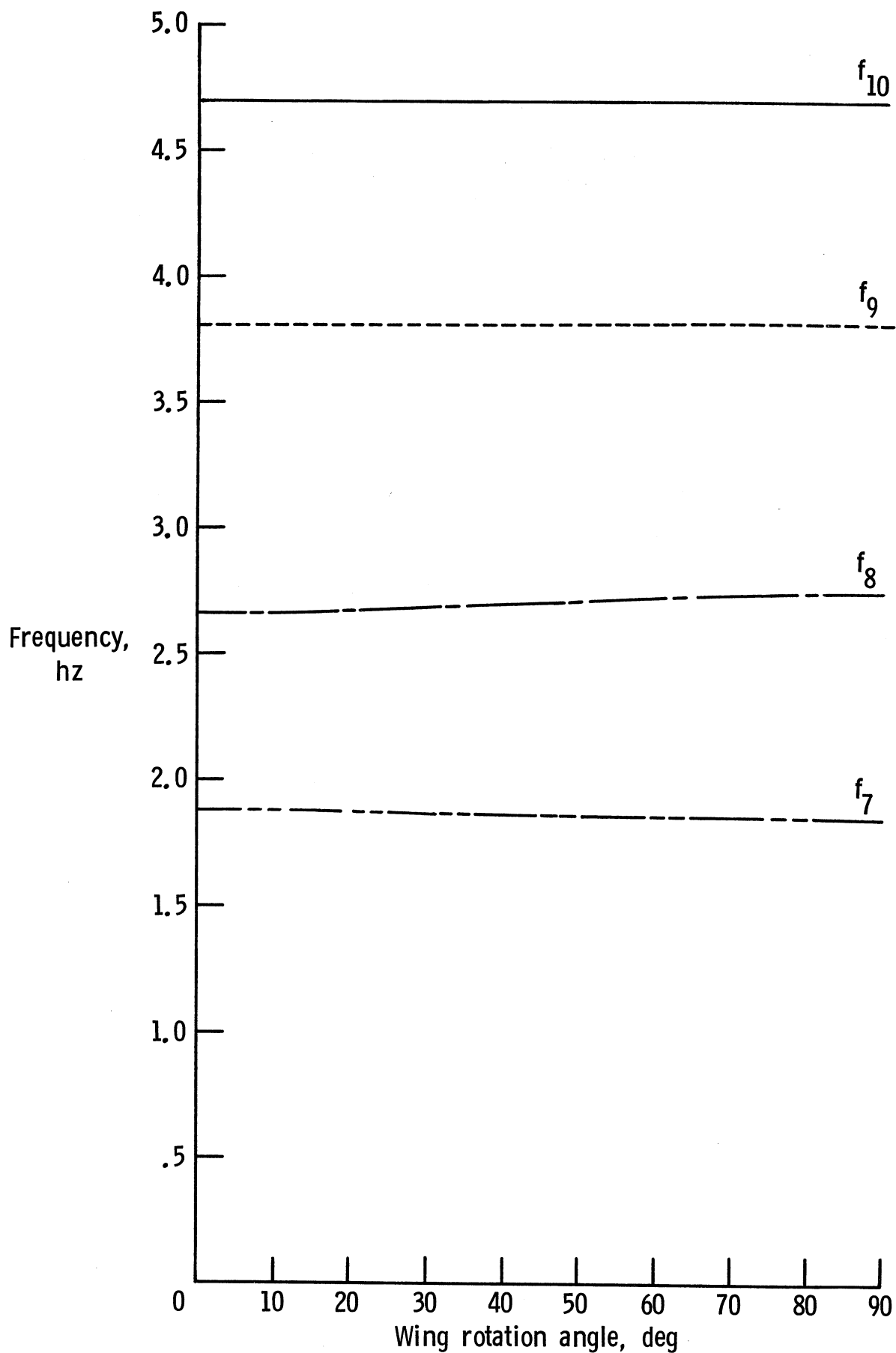


Figure 5. Variation in the gravity gradient stabilized space-station frequencies due to rotation of the solar wing arrays.

Figure 6

VARIATION IN GRAVITY GRADIENT STABILIZED STATION MASS MOMENTS  
OF INERTIA DUE TO ROTATION OF THE SOLAR WING ARRAYS

The variation in the principal mass moments of inertia,  $I_{xx}$ ,  $I_{yy}$  and  $I_{zz}$ , and products of inertia,  $I_{xy}$ ,  $I_{xz}$ , and  $I_{yz}$ , are shown as a function of wing rotation angle in figure 6. The mass moments of inertia of the complete station are considerably larger than the inertia for the station without all of the components added;  $I_{xx}$  is about 12 times as large,  $I_{yy}$  is about 1.6 times as large, and  $I_{zz}$  is about 3.1 times as large. As with the frequencies, there is not a great deal of variation in the space-station mass moments of inertia as the wings are rotated. The largest variation in a principal moment of inertia, 6.8%, occurs for  $I_{yy}$ .

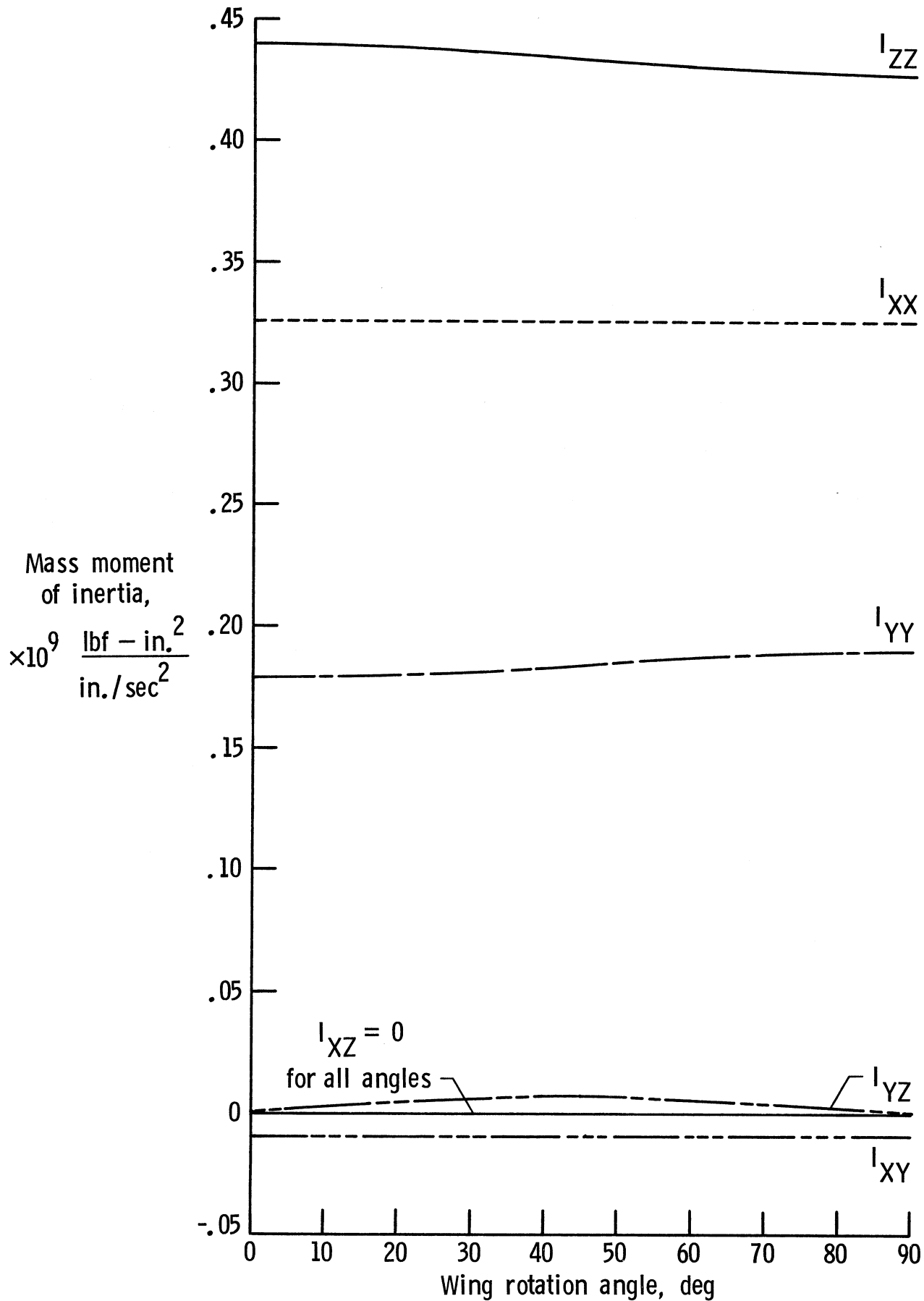
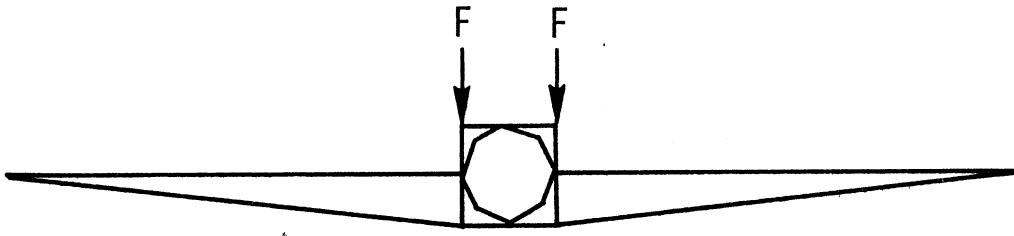


Figure 6. Variation in gravity gradient stabilized station mass moments of inertia due to rotation of the solar wing arrays.

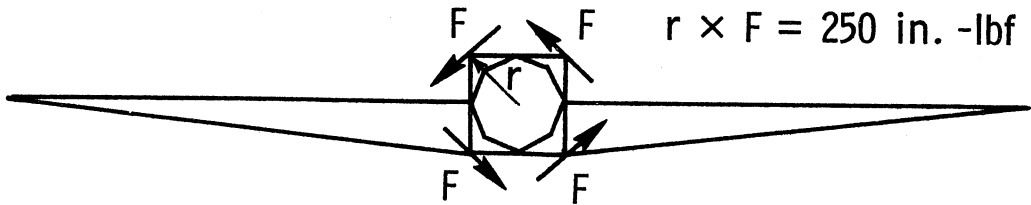
## Figure 7

### SOLAR WING ARRAY GEOMETRY

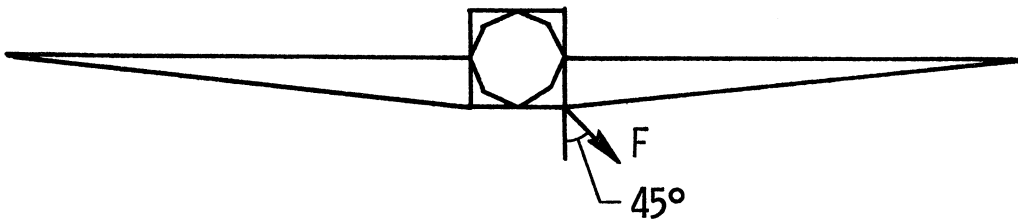
The solar wing array used for the strut failure studies is shown in figure 7. The solar array support truss is a four longeron single laced orthogonal tetrahedral truss. The truss supports twelve deployable solar array modules (six on each side) and is sized to provide 75 kw of power to the space-station. The wing is attached to a rotary joint by a transition structure and the rotary joint is connected to the cantilever support by another transition structure. The support truss has 14 ft square bays and the deployable solar arrays have a length of 66 ft. The total length of the wing array is 182 ft and the total width is 146 ft.



a. Load applied in negative Z direction ( $F = 5 \text{ lbf}$ )



b. Torque applied about the X axis (total torque =  $1000 \text{ in. -lbf}$ )



c. Load applied at minus  $45^\circ$  from the Y axis ( $F = 10 \text{ lbf}$ )

Figure 7. Solar wing array geometry.



Table IV  
FREQUENCIES AND MODE SHAPES OF ORTHOGONAL  
TETRAHEDRAL TRUSS WING

Table IV summarizes the first five cantilever modes and frequencies for the complete solar wing array. The properties of the struts making up the array support truss are the same as discussed in the narrations for figures 2 and 3. The rotary joint mass was assumed to be 2000 lbm, and the mass of the nodal joints and individual solar array modules were also included in the model. The fundamental mode for the cantilever wing array is first torsion about the x axis at a frequency of .599 hz. This compares very favorably with the first torsion frequency for the core-platform space-station with modules, being only 0.8% less.

TABLE IV  
 FREQUENCIES AND MODE SHAPES OF ORTHOGONAL TETRAHEDRAL TRUSS WING

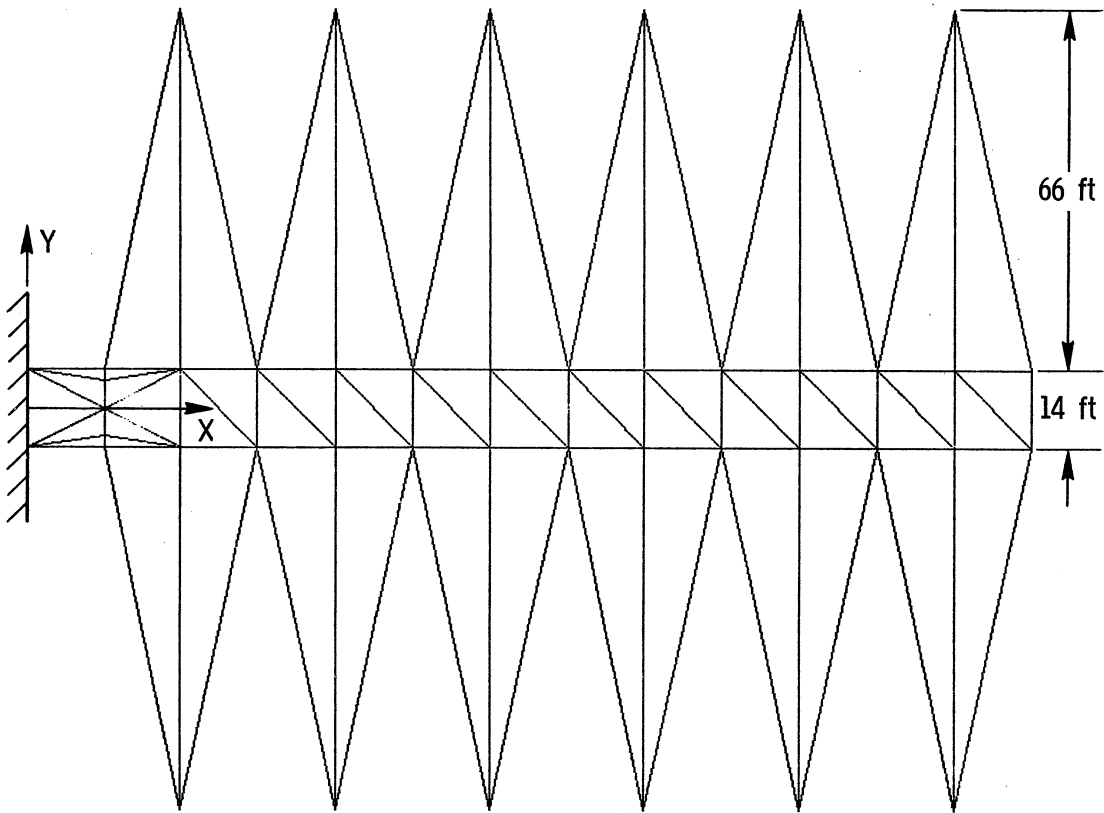
Mode Number	Frequency, hz	Shape
1	.599	1st torsion about X
2	.671	1st bending about an axis 45° from the Z
3	.735	1st bending about Y
4	1.21	2nd torsion about X
5	1.38	3rd torsion about X

## Figure 8

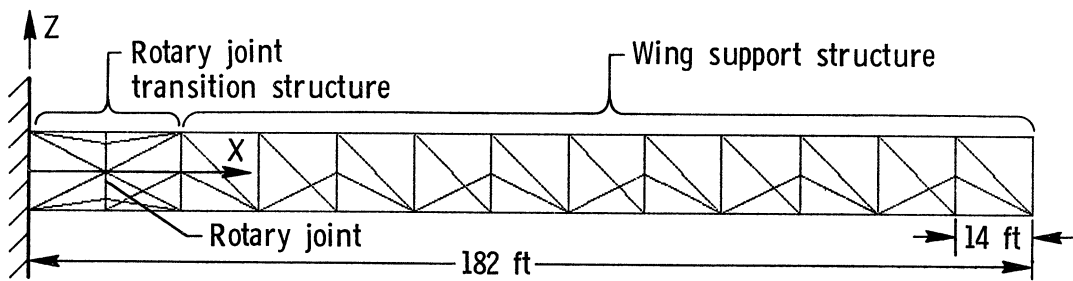
### THREE LOADING CONDITIONS APPLIED AT SOLAR WING ARRAY TIP

In this study, the three loading conditions shown in figure 8 were applied at the tip of the solar wing array. The first loading, shown in figure 8a, is a 10 lbf load applied at the wing tip in the minus Z direction. This will cause the loads in all four of the truss longerons to be of equal magnitude, with two in compression and two in tension. The force arrangement shown in figure 8b causes a torque of 1000 in-lbf to be applied at the tip of the wing. The applied tip loading shown in figure 8c will cause most of the axial forces in the truss to be carried by only two of the four longerons.

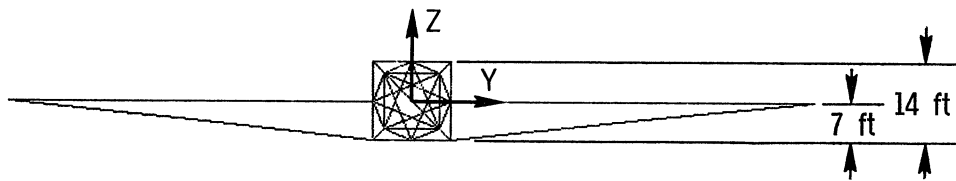
In preparing for the strut failure analysis, each of the three loading conditions described in figure 8 were applied separately to the wing model, and the wing deflection and member forces were calculated. The Euler buckling criteria given by,  $P_{CR} = \pi^2 EI/L^2$ , was applied to all members in the model to determine which two members (one in the array support truss and one in the gimbal transition truss) were closest to their critical load. The maximum load or torque which could be applied at the tip was calculated for each load case based on buckling of the appropriate critical member.



a. View of X - Y plane



b. View of X - Z plane



c. View of Y - Z plane

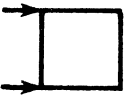
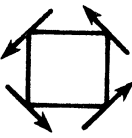
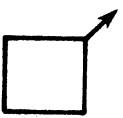
Figure 8. Three loading conditions applied at solar wing array tip.

Table V

FULL WING MODEL RESPONSE TO THREE APPLIED LOADING CONDITIONS

Table V summarizes the response of the full wing model to the three tip loading conditions described in figure 8. The tip displacement, critical member locations for both the transition truss and the support truss, and the maximum allowable applied tip load or torque are given for each case. The location of the critical members are given in the next figure and are discussed in more detail there. The maximum allowable load or torque which can be applied at the tip of the wing is based on failure of the critical member given in parentheses.

TABLE V  
 FULL WING MODEL RESPONSE TO THREE APPLIED LOADING CONDITIONS

Load Type	Tip Displacement (Node 160), in.	Critical Member Location		Maximum Allowable Tip Load or Torque
		Transition Truss	Support Truss	
 (See Fig. 8a)	-.0861	B	A	410 lbf (A)
 (See Fig. 8b)	.0038	C	D	286,000 in-lbf (D)
 (See Fig. 8c)	-.0845	B	A	324 lbf (A)

## Figure 9

### LOCATION OF CRITICAL MEMBERS AND TIP DISPLACEMENT MEASUREMENT POINT FOR SOLAR WING ARRAY

The location of the members which were removed for the strut failure analysis are shown in figure 9. The location of Node 160, which is the point where the tip deflection was measured, is also shown in the figure. In this investigation, for each of the three different loading conditions two critical members were identified; one in the rotary joint transition truss and one in the wing support truss. Thus, two cases were analyzed for each loading condition; one where the critical transition truss member is removed, and one where the critical wing support truss member is removed. The critical members were removed from the model one at a time, and the modes and frequencies of the wing were recalculated. The tip loads were also applied to the wing with the critical members removed and new deflections and maximum allowable loads or torque calculated. In all cases, the type of loading applied when the critical member was removed was the same type of loading which was applied to identify that particular critical member.

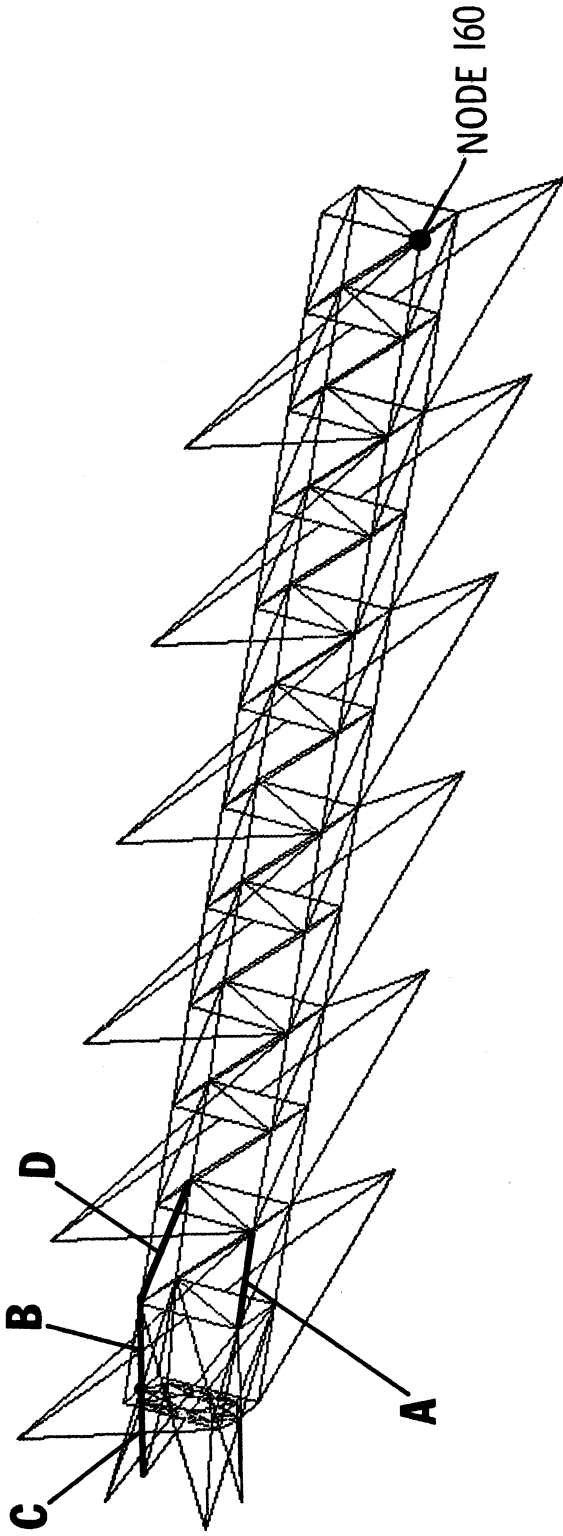


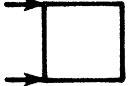
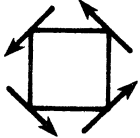
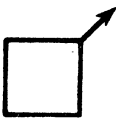
Figure 9. Location of critical members and tip displacement measurement point for solar wing array.



Table VI  
WING STRUT-FAILURE RESULTS

Table VI summarizes the results of the wing strut-failure analysis for the three types of tip loading. Loss of the critical members in the support truss, rather than the transition truss, cause the greater loss of stiffness (in terms of frequency) and strength (in terms of maximum allowable tip load or torque) in the wing array. For the loading condition shown in figure 8a and with critical member A removed from the model, there is a 47% reduction in the allowable tip load. For the loading condition shown in figure 8c and member A removed, there is a 50% reduction in the allowable tip load. The fundamental cantilever frequency is reduced by 23%, to .464 hz, when member A is removed from the model. For the loading condition shown in figure 8b, and the critical diagonal member D removed, there is a 50% reduction in the maximum allowable tip torque to 143,000 in-lbf and a 10.4% reduction in the fundamental cantilever frequency to .537 hz.

TABLE VI  
WING STRUT FAILURE RESULTS

Load Type	Critical Member Removed*	Tip Displacement (Node 160), in.	Frequency, hz					Maximum Allowable Tip Load or Torque
			f <sub>1</sub>	f <sub>2</sub>	f <sub>3</sub>	f <sub>4</sub>	f <sub>5</sub>	
	A	-.138	.464	.667	.686	1.20	1.37	219 lbf
	B	-.100	.556	.667	.716	1.19	1.36	316 lbf
	C	.00457	.578	.655	.726	1.20	1.37	285 000 in-lbf
	D	.00400	.537	.671	.722	1.19	1.36	143 000 in-lbf
	A	-.158	.464	.667	.686	1.20	1.37	162 lbf

\* See Figure 9 for member locations.

## CONCLUDING REMARKS

This report describes two space-station configurations which could be erected using orthogonal tetrahedral trusses. One objective of the investigations described in this report was to determine the dynamic characteristics (frequencies, mode shapes, and mass moments of inertia) of the space-stations with and without nonstructural components (modules, radiators, etc.). A second objective was to assess the structural behavior of a solar wing array after critical members in the wing had failed.

Both space-stations were able to meet the set stiffness requirement (fundamental frequency greater than .4 hz) when nonstructural components were not included in the configurations. The gravity gradient stabilized station structural characteristics, however, were much more sensitive to the addition of nonstructural components than the central platform space-station. The reason for this is that the keel is much more flexible (both in bending and torsion) than the central platform. Adding 200,000 lbm of nonstructural mass to the central platform space-station resulted in only a 10% decrease in the fundamental frequency to .504 hz; whereas in the gravity gradient stabilized space-station, the addition of 300,000 lbm caused a 63% reduction in the fundamental frequency to .187 hz. The central platform space station had approximately 100 000 lbm less nonstructural mass than the gravity gradient stabilized station. Adding another 100 000 lbm to the central platform, however, should not result in a significant decrease in the fundamental frequency of .504 hz since the central platform acts as a node (point of zero movement) for this mode.

The mass of both space-stations were dominated by the modules, radiators, OTV hangers, etc. rather than the solar arrays and truss structures. The addition of the various nonstructural components causes large changes in both space-station mass and moments of inertia. This will have an effect on the rigid body dynamics,

center-of-gravity and center-of-pressure locations, and thus the controllability of the space-station.

Studies of the gravity gradient space-station configuration showed that variations in frequencies and mass moments of inertia were very slight as the solar wing arrays were rotated.

The final studies showed that a catastrophic structural failure does not occur in the solar wing array if a critical member in the support truss fails. In the worst case studied, failure of a critical longeron resulted in only a 50% reduction in the load carrying capability of the wing and a 23% reduction in the fundamental frequency. The redundancy provided by the orthogonal tetrahedral truss design would prevent single point failures in the space-station structure.

## REFERENCES

1. Schock, R. W.: Solar Array Flight Experiment (SAFE). Large Space Systems Technology - 1981. NASA CP-2215, Part 2, 1981, pp. 881-891.
2. Dorsey, John T.; and Bush, Harold G.: Dynamic Characteristics of a Space-Station Solar Wing Array. NASA TM-85780, 1984.
3. Mikulas, Martin M., Jr.; Bush, Harold G.; Wallsom, Richard E.; Dorsey, John T.; and Rhodes, Marvin D.: A Manned-Machine Space-Station Construction Concept. NASA TM-85762, 1984.
4. Noor, Ahmed K.; and Anderson, C. M.: Analysis of Beam-Like Lattice Trusses. Comp. Meth. in Appl. Mech. and Eng., Vol. 20, 1979, pp. 53-70.

1. Report No. NASA TM-86260	2. Government Accession No.	3. Recipient's Catalog No.	
4. Title and Subtitle Structural Performance of Orthogonal Tetrahedral Truss Space-Station Configurations		5. Report Date July 1984	6. Performing Organization Code 506-53-43-01
		8. Performing Organization Report No.	
7. Author(s) John T. Dorsey		10. Work Unit No.	
9. Performing Organization Name and Address NASA Langley Research Center Hampton, VA 23665		11. Contract or Grant No.	
		13. Type of Report and Period Covered Technical Memorandum	
12. Sponsoring Agency Name and Address National Aeronautics and Space Administration Washington, DC 20546		14. Sponsoring Agency Code	
		15. Supplementary Notes	
16. Abstract  <p>This paper describes two 150 kw space-station configurations constructed with the orthogonal tetrahedral truss concept. One space-station consists of a large central platform and two rotating solar wing arrays and the other consists of a long central keel with two rotating arrays. The dynamic characteristics of each configuration are obtained with and without nonstructural components (habitation modules, radiators, fuel tanks, etc.) present. The variation in frequencies and mass moments of inertia due to rotation of the two solar wing arrays are given for the long keel (gravity gradient stabilized) space-station configuration. Finally, the structural performance of the solar wing array is assessed for cases when individual critical struts fail in the array support truss.</p>			
17. Key Words (Suggested by Author(s)) Space Station Structural Dynamics Critical Member Failure		18. Distribution Statement  Unclassified - Unlimited  Subject Category 18	
19. Security Classif. (of this report) Unclassified	20. Security Classif. (of this page) Unclassified	21. No. of Pages 37	22. Price A03